NEOPLASIA
www.neoplasia.com

Volume 24 Number 2 February 2022 pp. 109–119 109

Original Research

Selective BH3 mimetics synergize with BET inhibition to induce mitochondrial apoptosis in rhabdomyosarcoma cells

Ufuk Erdogdu [a,#]; Nadezda Dolgikh [a,#]; Stephanie Laszig [a]; Vinzenz Särchen [a]; Michael T. Meister [a]; Marek Wanior [c]; Stefan Knapp [b,c]; Cathinka Boedicker [a,*]

[a] Institute for Experimental Tumor Research in Pediatrics, Goethe-University Frankfurt, Komturstrasse 3a, Frankfurt 60528, Germany
[b] German Cancer Consortium (DKTK), Partner Site Frankfurt, Germany
[c] Institute of Pharmaceutical Chemistry, Goethe-University Frankfurt and Structural Genomics Consortium (SGC), Buchmann Institute for Molecular Life Sciences (BMLS), Frankfurt, Germany

Abstract

BH3 mimetics are promising novel anticancer therapeutics. By selectively inhibiting BCL-2, BCL-x_L, or MCL-1 (i.e. ABT-199, A-1331852, S63845) they shift the balance of pro- and anti-apoptotic proteins in favor of apoptosis. As Bromodomain and Extra Terminal (BET) protein inhibitors promote pro-apoptotic rebalancing, we evaluated the potential of the BET inhibitor JQ1 in combination with ABT-199, A-1331852 or S63845 in rhabdomyosarcoma (RMS) cells. The strongest synergistic interaction was identified for JQ1/A-1331852 and JQ1/S63845 co-treatment, which reduced cell viability and long-term clonogenic survival. Mechanistic studies revealed that JQ1 upregulated BIM and NOXA accompanied by downregulation of BCL-x_L, promoting pro-apoptotic rebalancing of BCL-2 proteins. JQ1/A-1331852 and JQ1/S63845 co-treatment enhanced this pro-apoptotic rebalancing and triggered BAK- and BAX-dependent apoptosis since a) genetic silencing of BIM, BAK or BAX, b) inhibition of caspase activity with zVAD.fmk and c) overexpression of BCL-2 all rescued JQ1/A-1331852- and JQ1/S63845-induced cell death. Interestingly, NOXA played a different role in both treatments, as genetic silencing of NOXA significantly rescued from JQ1/A-1331852-mediated apoptosis but not from JQ1/S63845-mediated apoptosis. In summary, JQ1/A-1331852 and JQ1/S63845 co-treatment represent new promising therapeutic strategies to synergistically trigger mitochondrial apoptosis in RMS.

Neoplasia (2022) 24, 109–119

Keywords: Apoptosis, BH3 mimetics, BET proteins, Rhabdomyosarcoma

Introduction

Rhabdomyosarcoma (RMS) is a frequent soft-tissue sarcoma in children and adolescents comprising two major subtypes, the alveolar subtype (ARMS) and the embryonal subtype (ERMS), which are classified by specific genetic alterations and phenotypes [1]. While the overall prognosis for RMS has steadily improved over the last years due to multimodal treatment, the prognosis for ARMS and ERMS patients suffering relapses is still poor, highlighting the need to develop new therapies [2].

Bromodomains (BRDs) are important epigenetic regulators of transcription by recognizing acetylated lysines of histones. The bromodomain and extra-terminal (BET) proteins consist of BRD2, BRD3, BRD4 and BRDT and belong to the BRD subfamily II. In recent years, especially BRD4 has become a well-characterized protein influencing lineage-specific genes or promoting gene-specific transcription [3]. Some cancer cells are highly dependent on BRD4, since oncogenes such as *MYC* are regulated

Abbreviations: ATCC, American Type Culture Collection; ARMS, alveolar rhabdomyosarcoma; mBCL-2, murine BCL-2; BRD, bromodomain; BET protein, Bromo- and Extra-Terminal protein; BRD4, bromodomain-containing protein 4; CI, combination index; ERMS, embryonal rhabdomyosarcoma; EV, empty vector; FCS, fetal calf serum; MTT, 3-(4,5-dimethylthiazol-2-yl)-2,5-diphenyltetrazolium bromide; PI, propidium iodide; PBMC, peripheral blood mononuclear cell; RMS, rhabdomyosarcoma; zVAD.fmk, *N*-benzyloxycarbonyl-Val-Ala-Asp-fluoromethylketone.

* Corresponding author.
E-mail address: c.boedicker@kinderkrebsstiftung-frankfurt.de (C. Boedicker).
shared first authorship

Received 23 March 2021; received in revised form 12 November 2021; accepted 23 November 2021

https://doi.org/10.1016/j.neo.2021.11.012

by enhancers and super-enhancers harboring high levels of acetylated histones resulting in BRD4 recruitment and transcriptional activation [4, 5]. Consequently, BET inhibitors (e.g. JQ1) have emerged as potent novel anticancer drugs in various tumor entities. BET inhibitors displace BET proteins from acetylated chromatin, thereby interfering with BET mediated transcriptional activation [3]. So far, results of clinical trials with BET inhibitors show limited efficiency in various cancer types, in particular due to dose limiting toxicities and early onset of resistance. Thus, pan-BET inhibition alone is not sufficient to induce cell death [5–7]. However, BET inhibition has been shown to synergize with various chemotherapeutics to induce apoptosis in many cancer types [5, 6, 8].

Apoptosis is a form of programmed cell death and can be divided into mitochondrial (intrinsic) and death receptor (extrinsic) apoptosis. The intrinsic apoptotic pathway is tightly regulated by the balance of the BCL-2 protein family, which include the pro-apoptotic BH3-only proteins (e.g. BIM, NOXA, BMF), the multidomain effector proteins BAK and BAX as well as the anti-apoptotic proteins (e.g. BCL-2, BCL-x_L, or MCL-1) [9,10]. In general, BAK and BAX are neutralized by binding to anti-apoptotic BCL-2 proteins. BH3-only proteins can activate BAK and BAX either directly or indirectly, by displacing them from the anti-apoptotic BCL-2 proteins. As a result, activated BAK and BAX oligomerize to form pores in the mitochondrial outer membrane resulting in mitochondrial outer membrane permeabilization and release of mitochondrial proteins into the cytoplasm including cytochrome c. Upon cytochrome c release, the apoptosome is formed resulting in caspase activation and execution of apoptosis [9,10].

Since the balance of BCL-2 proteins is crucial for the induction of apoptosis [10], BH3 mimetics (i.e. ABT-199, A-1331852, S63845) selectively inhibiting anti-apoptotic BCL-2 proteins (BCL-2, BCL-x_L, or MCL-1) have been developed [11–14]. In many cancer types including RMS the effect of BH3 mimetics as single treatment is limited [15, 16]. However, previous studies have highlighted the potential of BH3 mimetics in combination therapies in RMS *in vitro* [17, 18]. Since our previous studies highlighted the potential of BET inhibition to rebalance BCL-2 proteins in favor of apoptosis [6, 19], we hypothesized that RMS cells are highly vulnerable to a dual treatment using BET inhibitors and BH3 mimetics.

Materials & methods

Cell culture and chemicals

RMS cell lines were obtained from the American Type Culture Collection (ATCC) (Manassas, VA, USA) or the Deutsche Sammlung von Mikroorganismen und Zellkulturen GmbH (Braunschweig, Germany) and cultivated in DMEM GlutaMAXX medium or RPMI 1640 medium (Life Technologies Inc., Eggenstein, Germany) with addition of 1% Penicillin/Streptomycin and 1 mM sodium pyruvate 10%-20% fetal calf serum (FCS), and incubated at 37°C with 5% CO_2 in air. Peripheral blood mononuclear cells (PBMCs) were obtained from buffy coat from heathy blood donors by the Deutsches Rotes Kreuz Blutspendedienst Frankfurt. JQ1 was kindly provided by S. Knapp and M. Wanior (Frankfurt, Germany). The BH3 mimetics ABT-199, A-1331852, S63845 selectively targeting BCL-2, BCL-x_L, or MCL-1 were obtained from Selleck Chemicals (Houston, TX, USA) and the broad-range caspase inhibitor N-benzyloxycarbonyl-Val-Ala-Asp-fluoromethylketone (zVAD.fmk) from Bachem (Heidelberg, Germany). All inhibitors were dissolved in dimethyl sulfoxide (DMSO) at variable stock concentrations.

Determination of metabolic activity, cell death and clonogenic growth

Metabolic activity was measured by MTT (3-(4,5-dimethylthiazol-2-yl)-2,5-diphenyltetrazolium bromide) assay as described by manufacturer's instructions (Roche Diagnostics, Mannheim, Germany). Cell death was either determined by propidium iodide (PI)/Hoechst 33342 double staining (both purchased from Sigma Aldrich) using fluorescence-based microscopic analysis or, alternatively, flow cytometric analysis (FACS Canto II, BD Biosciences, Heidelberg, Germany) of PI-stained nuclei. For clonogenic growth assay, cells were seeded in a 24-well plate at a density of 30000 cells/cm^2 and allowed to attach overnight, treated the next day for 24 hours as indicated and afterwards detached by trypsin and counted. In dependence of the cell line, 100-400 cells/well were reseeded in a six-well plate. Eight days after reseeding, medium was substituted with fresh medium and colonies were stained after 12-14 days with crystal violet solution (0.5% crystal violet, 30% ethanol, 3% formaldehyde). The percentage of colonies relative to solvent-treated controls was calculated after manual counting of the colonies.

Determination of caspase-3/-7 activity

To determine activation of caspase-3 and -7 cells at a density of 15000 cells/cm^2 were seeded in a 96-well plate and allowed to attach overnight. The next day cells were treated as indicated for 18 hours, followed by addition of Cell Event Caspase-3/-7 Green Detection Reagent (Life Technologies Inc.) to each well at a final concentration of 2 µM followed by incubation for six hours. Next, the cells were stained with Hoechst 33342 and percentage of cells with caspase-3/-7 activation was calculated using fluorescence-based microscopic analysis.

Transduction

Transduction of RMS cells was performed as described previously [20]. In summary, Phoenix packaging cells were transfected with 20 µg virus using calcium phosphate transfection as described previously [20]. For murine BCL-2 overexpression murine stem cell virus (PMSCV, Clontech, Mountain View, CA, USA) containing mBCL-2 or empty vector (EV) and Lipofectamine 2000 (Life Technologies, Inc.) were used and selected with 0.5 mg/ml G418 (Carl Roth, Karlsruhe, Germany).

For BCL-x_L overexpression RH30 and RH36 cells were transiently transfected with 1 µg/ml pMIG plasmid containing empty vector or BCL-x_L (addgene (Plasmid #8790)) using Lipofectamine 200 (Invitrogen) following the manufacturer's instructions.

RNA interference

For transient siRNA knockdown cells were seeded at a density of 20000 cells/cm^2 and reversely transfected with 20 nM SilencerSelect siRNA (Life Technologies Inc.) using Lipofectamine RNAiMAX (Invitrogen) and OptiMEM (Life Technologies). BAK was targeted with constructs s1880 and 1881, BAX with s1888 and s1900, BIM with constructs s195012, s223065 and NOXA with constructs s10709 and s10710. Construct s4390843 was used as non-silencing control siRNA. For knockdown, Lipofectamine RNAiMAX and siRNA were separately diluted in OptiMEM and the two dilutions were then combined and incubated for 20 minutes at room temperature and distributed on top of the cells. Eight hours after transfection medium was exchanged.

Western blot analysis

Western blot analysis was conducted as described before [21] using the following antibodies: mouse anti-α-Tubulin (Calbiochem, Darmstadt, Germany; Cat. No. CP06-100UG) mouse anti-β-Actin (Sigma Aldrich, Germany; Cat. No. A5441), mouse anti-GAPDH (HyTest, Turku, Finland; Cat. No. 5G4-6C5), mouse anti-VINCULIN (Sigma Aldrich, Germany, Cat. No. V9131-100UL), rabbit anti-BIM, rabbit anti-BCL-x_L, rabbit anti-BAX, mouse anti-MCL-1, mouse anti-NOXA, rabbit anti-BAK-NT (Merck, Darmstadt, Germany; Cat. No. 06-599, 06-536) and mouse anti-BCL-2

(Dako, Santa Clara, CA, USA; Cat. No. M088701-2). For detection, goat anti-rabbit, goat anti-mouse and goat anti-rat IgG conjugated to horseradish peroxidase (Santa Cruz Biotechnology, Santa Cruz, CA, USA; Cat. No. SC-2004, SC-2005, SC-2006) and enhanced chemiluminescence (Amersham Biosciences, Freiburg, Germany) or infrared dye-labelled donkey anti-rabbit and donkey anti-mouse IgG secondary antibodies and infrared imaging (Odysee Imaging System, LI-COR Biosciences, Bad Homburg, Germany) were used. Representative blots of at least two independent experiments are shown.

BAK and BAX activation

Immunoprecipitation of active BAK and BAX complexes was performed as previously described [19]. In brief, RMS cells were lysed in CHAPS lysis buffer (1% CHAPS: 10 mM HEPES (pH 7.4); 150 mM NaCl) with protease inhibitor cocktail (Roche, Grenzach, Germany). For IP 2 µg/mL mouse anti-BAX 6A7 antibody (Sigma, Germany) or 2 µg/mL mouse anti-BAK antibody (Calbiochem, San Diego, CA, USA) and 10 µL pan-mouse IgG Dynabeads were added to 1000 µg protein and incubated at 4°C for 24 hours. Next, the precipitate was washed three times with CHAPS buffer. For detection of activated BAX and BAK expression Western blot analysis was performed with either rabbit anti-BAX antibody (Cell Signaling, Beverly; Cat. No. 2772S) or rabbit anti-BAK NT antibody (Merck, Darmstadt, Germany; Cat. No. 06-536) as following antibody.

3D multicellular tumor spheroid model

Rhabdomyosarcoma cells, RH30 and RH36, were seeded in ultra-low attachment 96-well plates (Corning, NY, USA) in 100 µL total volume to generate one spheroid per well, as described previously [22]. The initial spheroids consisted of 2500 cells per well for RH30 and 5000 cells per well for RH36 cells. Cell numbers were empirically determined to achieve similar spheroid size on the day of treatment. After seeding in respective cell culture medium, the plate was centrifuged at 1000 x g for 10 minutes and incubated for 3 days before treatment. On the day of treatment JQ1, A1331852 or S63845 were added alone or in combination to reach a final concentration of 0.5, 0.25 and 0.25 µM, in a total volume of 200 µL per well. To assess cell death, tumor spheroids were stained with Hoechst, for 1 hour (final concentration 20 µg/mL) and PI for 30 minutes (final concentration 2 µg/mL). Image acquisition was performed using an ImageXpress Micro XLS Widefield Analysis System (Molecular Devices, Sunnydale, CA) and analysis using MetaXpress with a custom module algorithm (Version 6.5.4.532, Molecular Devices, Sunnydale, CA) and FIJI (ImageJ version 1.53c) [23].

Statistical analysis

For comparison of two samples calculation of statistical significance two-tailed, two sample, equal variance student's t-test was used. To compare more than two samples we performed one-way ANOVA followed by Dunnet's multiple comparisons test using GraphPad Prism® (version 7.03, GraphPad Software, San Diego, CA). To analyze drug interaction of JQ1 with A-1331852 or S63845, Bliss synergy score was ascertained using Synergy Finder [24]. For this score values > 1 signify synergism, whereas values < -1 signify antagonism and everything in between additivity [24].

Data availability

Primary data are available on request from the authors.

Results

JQ1 and BH3 mimetics synergize to induce cell death in RMS cells

To characterize the sensitivity of RMS cells towards single treatment with the BH3 mimetics, MCL-1 inhibitor (MCL1i) S63845, the Bcl-x_L inhibitor (Bcl-x_Li) A-1331852 and the BCL-2 inhibitor (BCL-2i) ABT-199, we performed dose-dependent experiments in two representative ERMS cell lines (RD, RH36) and two representative ARMS cell lines (RH30, RH41). All tested cell lines showed moderate cell death induction as indicated by PI-positive cells in response to single treatment with the three BH3 mimetics (Supplementary Figure 1). Encouraged by our previous data that RMS cells are sensitive to combination treatments with the BET inhibitor JQ1 [6, 19], we next treated the RMS cells with the BH3 mimetics in combination with JQ1 to induce cell death. Combination of JQ1 with either S63845, A-1331852 or ABT-199 synergistically induced cell death in a dose-dependent manner, as indicated by PI-positive cells and Bliss synergy score (Figure 1A, Supplementary Table 1). By calculating the Bliss synergy score, the strongest synergism could be identified upon JQ1/A-1331852 and JQ1/S63845 co-treatment (Supplementary Table 1). Interestingly, this synergistic effect points to some tumor selectivity as all three combinations did not induce cell death in peripheral blood mononuclear cells (PBMCs) as indicated by less than 20% PI-positive cells upon combination treatment (Supplementary Figure 2). Since the combinations of JQ1 with either A-1331852 or S63845 turned out to be most potent in RH36 and RH30 cells, we decided to focus on these combinations in RH36 and RH30 cells. To test both co-treatments in a pre-clinical test model displaying physiologically relevant 3D cell-cell interactions of *in vivo* tumors, we next assessed the effect of JQ1/A-1331852 and JQ1/S63845 co-treatment in 3D spheroid models. JQ1/A-1331852 and JQ1/S63845 co-treatment induced significantly more PI positive cells compared to control in RH36 and RH30 spheroids. Furthermore, both co-treatments induced significantly more PI positive cells compared to the single treatments in RH30 cells (Supplementary Figure 3). In order to investigate the time dependency of JQ1/A-1331852- and JQ1/S63845-mediated cell death induction, we treated RH36 and RH30 cells with 0.5 µM JQ1 and/or 0.25 µM S63845 and/or A-1331852 and measured PI-positive cells from 24 to 96 hours (Figure 1B). Both combinations potently induced cell death in a time-dependent manner as indicated by more than 60% PI-positive cells after 72 and 96 hours, while single treatment with S63845 resulted in 18% PI-positive cells and single treatment with A-1331852 36% PI-positive cells after 96 hours (Figure 1B). In summary, JQ1/A-1331852 and JQ1/S638450 co-treatment induced cell death in a time- and dose-dependent manner.

JQ1 and S63845 or A-1331852 cooperate to reduce cell viability and inhibit colony formation

The effect of JQ1/A-1331852 and JQ1/S63845 co-treatment on RMS cells was further investigated in cell viability experiments measuring the metabolic activity after 72 hours. Importantly, JQ1 cooperated with A-1331852 and S63845 to reduce cell viability (Figure 2A). To study the long-term effects of JQ1/A-1331852 and JQ1/S63845 co-treatments, we next performed colony formation assays (Figure 2B). JQ1/A-1331852 and JQ1/S63845 co-treatment both significantly reduced colony formation in RH36 and RH30 cells compared to the untreated control and JQ1-treated RMS cells (Figure 2B).

JQ1 and S63845 or A-1331852 cooperate to induce caspase activation and caspase-dependent apoptosis

Since we wanted to characterize the molecular mechanisms of JQ1/A-1331852- and JQ1/S63845-mediated cell death, we next analyzed DNA

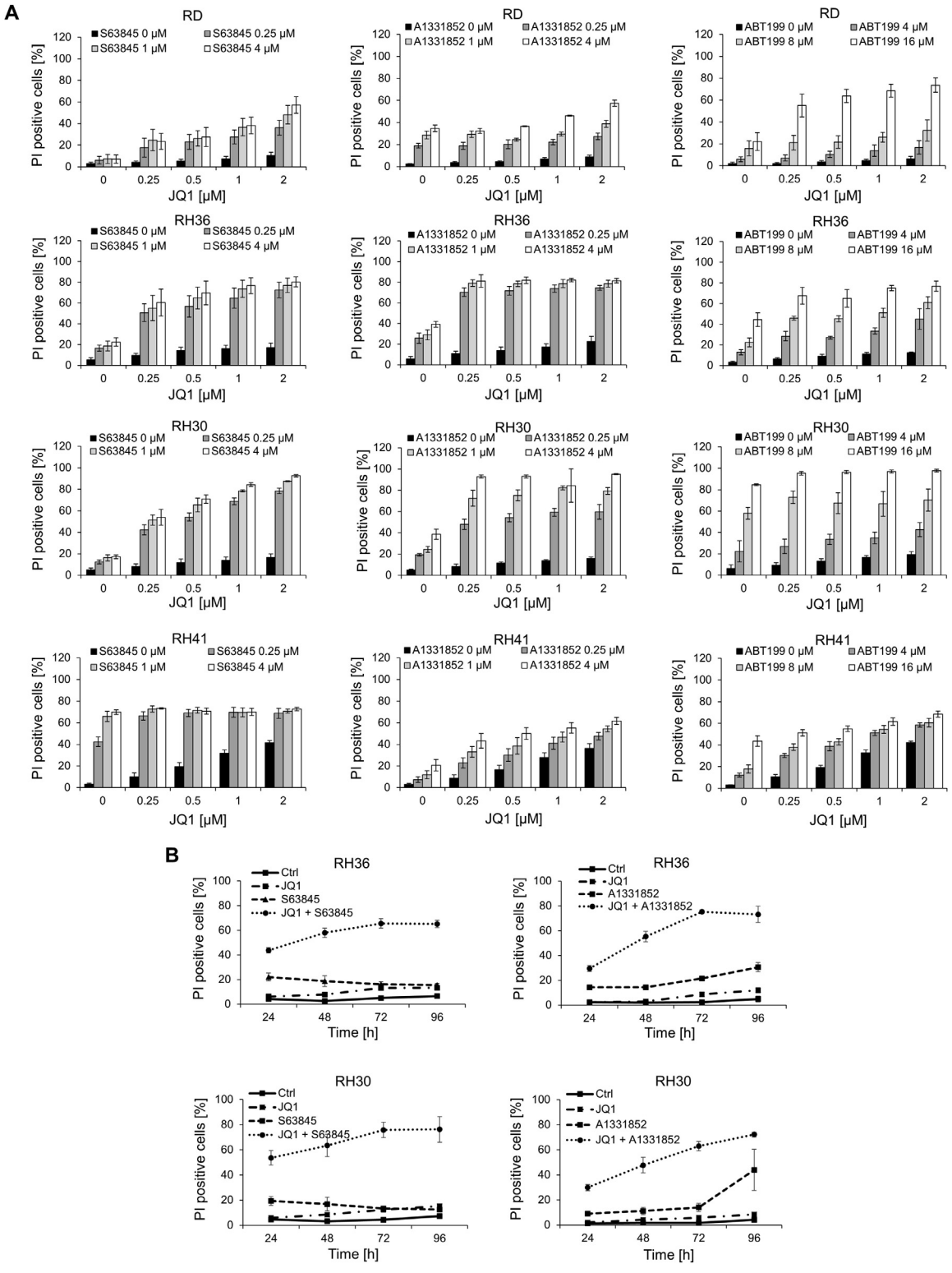

Fig. 1. JQ1 and BH3 mimetics synergize to induce cell death in RMS cells. RMS cell lines (RD, RH36, RH30 and RH41) were treated with the indicated concentrations of JQ1 and/or S63845 (MCL1i), A-1331852 (Bcl-x_Li) or ABT-199 (BCL-2i) for 72h. (A) Cell death was determined by analysis of PI/Hoechst staining using the ImageXpress Micro XLS system. Data are shown as mean and SD of at least three independent experiments performed in triplicate. (B) RMS cell lines were treated with 0.5 µM JQ1 and/or 0.25 µM S63845 (MCL1i) and/or A-1331852 (Bcl-x_Li) for the indicated time points and cell death was determined by analysis of PI/Hoechst staining using the ImageXpress Micro XLS system Data are shown as mean and SD of at least three independent experiments performed in triplicate.

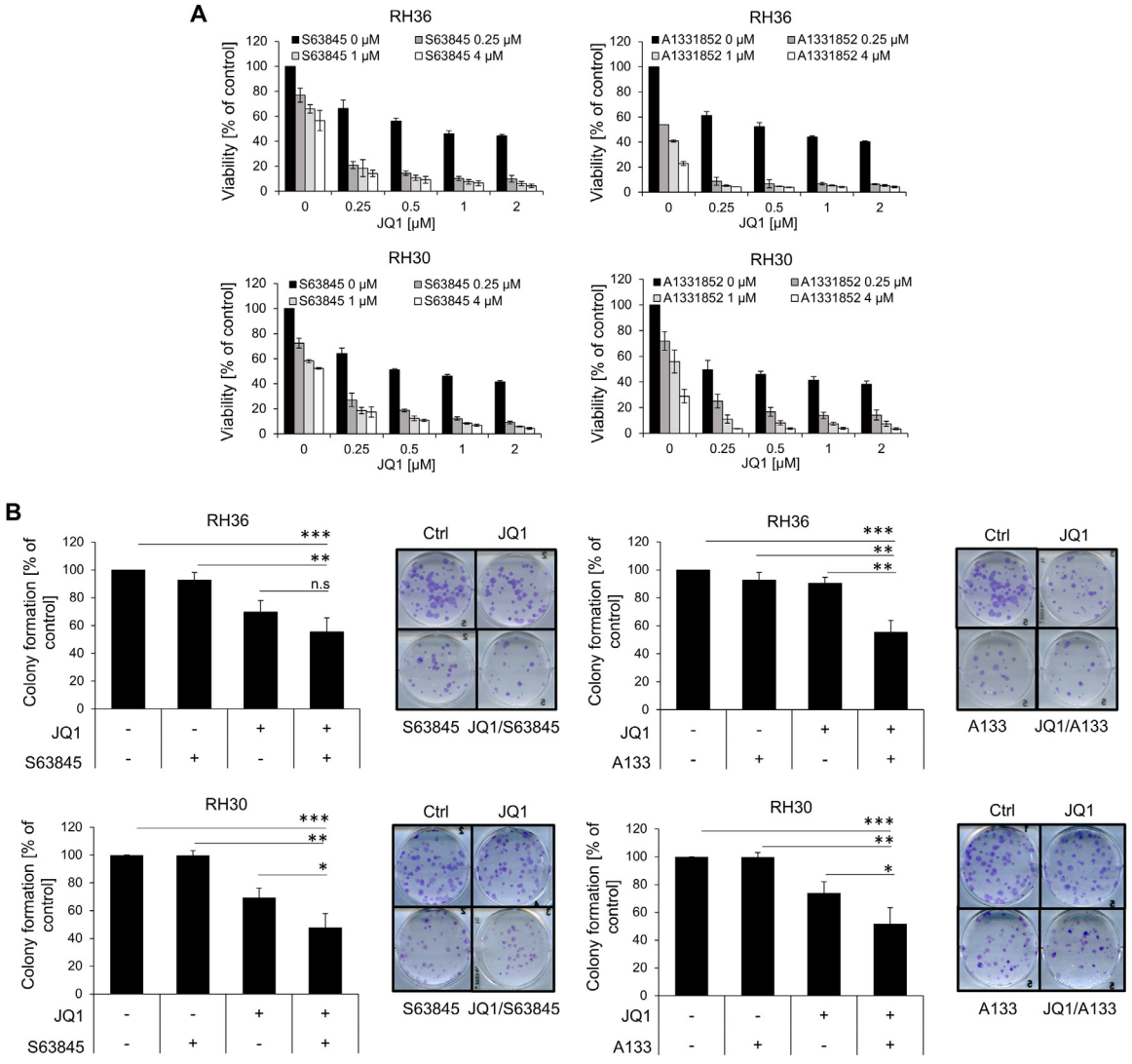

Fig. 2. JQ1 and S63845 or A-1331852 cooperate to reduce cell viability and inhibit colony formation. (A) Metabolic activity of RMS cells was detected by MTT assay. (B) RMS cells were treated with indicated concentrations of JQ1 and S63845 or A-1331852 for 24 hours and colony formation was assessed after 12 - 14 days by manual counting of crystal violet stained colonies. The number of colonies is displayed as percentage of solvent-treated controls (left panels) and representative images are shown (right panels). *p<0.1, **p<0.01, ***p<0.001 comparing JQ1/S63845 or JQ1/A-1331852 co-treated cells to either single treatments or control.

fragmentation and caspase activation, which are typical hallmarks of caspase-dependent apoptosis. JQ1/A-1331852 and JQ1/S63845 co-treatment induced significantly more DNA fragmentation in comparison to single treatments after 72 hours (Figure 3A). In addition, JQ1/A-1331852 and JQ1/S63845 co-treatment significantly increased caspase-3/-7 activation compared to single treatments after 24 hours (Figure 3B). The functional relevance of caspase activation for JQ1/A-1331852- and JQ1/S63845-induced cell death is underlined by experiments with the broad range caspase inhibitor zVAD.fmk significantly rescued RH36 and RH30 cells from JQ1/A-1331852- and JQ1/S63845-induced DNA fragmentation (Figure 3C). Taken together, these data show that JQ1/A-1331852 and JQ1/S63845 co-treatment induced caspase-dependent apoptosis.

JQ1/S63845- and JQ1/A-1331852-induced cell death is dependent on BAK and BAX

Mitochondrial apoptosis is tightly regulated by the pro-apoptotic multidomain proteins BAK and BAX that control mitochondrial membrane permeabilization by forming pores in the outer mitochondrial membrane. Therefore, we assessed BAK and BAX activation upon treatment with JQ1/A-1331852 and JQ1/S63845 co-treatment, using conformation-specific antibodies. While JQ1, A-1331852 or S63845 resulted in minor activation of BAX both co-treatments resulted in pronounced increase of activated BAX protein levels. In contrast, A-1331852 and S63845 single treatment as well as JQ1/A-1331852 and JQ1/S63845 co-treatment resulted in increase of activated BAK protein levels. Besides, A-1331852 and JQ1/A-1331852 co-treatment resulted in higher levels of activated BAK levels compared to S63845 or JQ1/S63845 (Figure 4A). To investigate the functional relevance of BAK and BAX activation, we performed individual knockdown of either BAK or BAX, which was confirmed by Western blotting (Figure 4B, 4D). Individual knockdown of either BAK or BAX both significantly rescued from JQ1/S63845- or JQ1/A-1331852-mediated apoptosis (Figure 4C, 4E). Of note, JQ1/S63845-induced cell death was rescued more efficiently by genetic silencing of BAK as indicated by a significant reduction of RH36 and RH30 PI-positive cells from 60% to 23% and 59% to 22%. In contrast, upon JQ1/A-1331852 treatment, BAK knockdown only reduced cell death

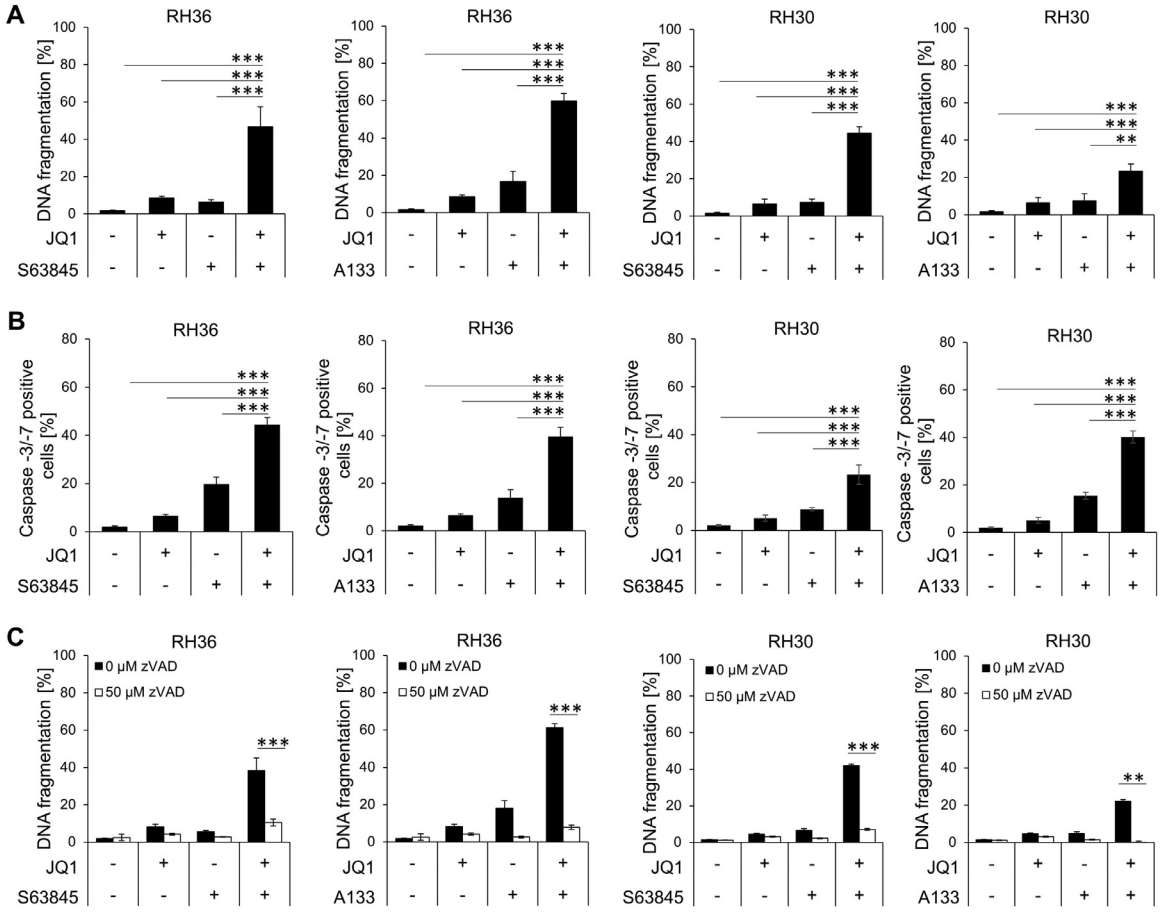

Fig. 3. JQ1 and S63845 or A-1331852 cooperate to induce caspase activation and caspase-dependent apoptosis. (A) RMS cell lines were treated with 0.5 µM JQ1 and/or 0.25 µM S63845 (MCL1i) and/or A-1331852 (Bcl-x_Li) for 72 h and apoptosis was determined by analysis of DNA fragmentation of PI-stained nuclei using flow cytometry. Mean and SD of three experiments performed in triplicate are shown. **p<0.01, ***p<0.001 comparing JQ1/S63845 or JQ1/A-1331852 co-treated cells to either single treatments or control. (B). RMS cell lines were treated with 0.5 µM JQ1 and/or 0.25 µM S63845 (MCL1i) and/or A-1331852 (Bcl-x_Li). Caspase activation was determined by Cell Event Caspase-3/-7 Green Detection Reagent and ImageXpress Micro XLS system. Data represent the mean ± SD of three independent experiments, performed in triplicates; *p<0.05; **p<0.01 comparing JQ1/S63845 or JQ1/A-1331852 co-treated cells. (C) RMS cell lines were treated with 0.5 µM JQ1 and/or 0.25 µM S63845 (MCL1i) and/or A-1331852 (Bcl-x_Li) in the absence and presence of 50 µM zVAD.fmk for 72 h. Apoptosis was determined by analysis of DNA fragmentation of PI-stained nuclei using flow cytometry. Data represent the mean ±SD of three independent experiments, performed in triplicates; **p<0.01, ***p<0.001 comparing JQ1/S63845 or JQ1/A-1331852 co-treated cells in the absence and presence of 50 µM zVAD.fmk.

of RH36 and RH30 cells to 41% or 48% PI-positive cells, respectively (Figure 4C). BAX knockdown turned out to be more efficient in rescuing JQ1/A-1331852-mediated cell death compared to JQ1/S63845-mediated cell death in RH36 and RH30 cells (Figure 4E). However, the differences in the rescue effect of BAX knockdown upon both treatments were slightly less pronounced compared to the effect seen after BAK knockdown (Figure 4C, 4E). Taken together, these results display that JQ1/S63845- and JQ1/A-1331852-mediated cell death is dependent on BAK and BAX.

JQ1/A-1331852 and JQ1/S63845 co-treatment differently regulate BIM and NOXA expression

To further investigate the molecular mechanisms of JQ1/A-1331852- and JQ1/S63845-mediated apoptosis, we next investigated the effects of both treatment combinations on the BCL-2 protein family. JQ1 upregulated the pro-apoptotic BCL-2 proteins BIM and NOXA, while downregulating anti-apoptotic BCL-x_L, thereby rebalancing the ratio of pro- and anti-apoptotic BCL-2 proteins towards apoptosis (Figure 5A, 5B). Interestingly, S63845 as well as JQ1/S63845 co-treatment reduced NOXA protein levels already after 6 hours (Figure 5B) and BIM proteins levels after 16 hours (Figure 5A). Furthermore, S63845 and JQ1/S63845 co-treatment resulted in slightly increased protein levels of MCL-1 in RH36 cells. A-1331852 single treatment decreased BCL-x_L protein levels after 16 hours, but did not affect NOXA protein levels (Figure 5A, 5B). In summary, the most prominent differences between both treatments are the observations that, S63845 and JQ1/S63845 co-treatment decreased NOXA protein levels, whereas JQ1 and JQ1/A-1331852 co-treatment increased NOXA protein levels after 6 hours (Figure 5A, 5B).

JQ1/A-1331852- and JQ1/S63845-mediated apoptosis is dependent on proapoptotic rebalancing of BCL-2 proteins

Next, we investigated the functional relevance of BIM and NOXA for JQ1/S63845- and JQ1/A-1331852-mediated apoptosis, since both co-treatments displayed different effects on BIM and NOXA protein expression. To this end, we performed siRNA knockdown experiments using two distinct

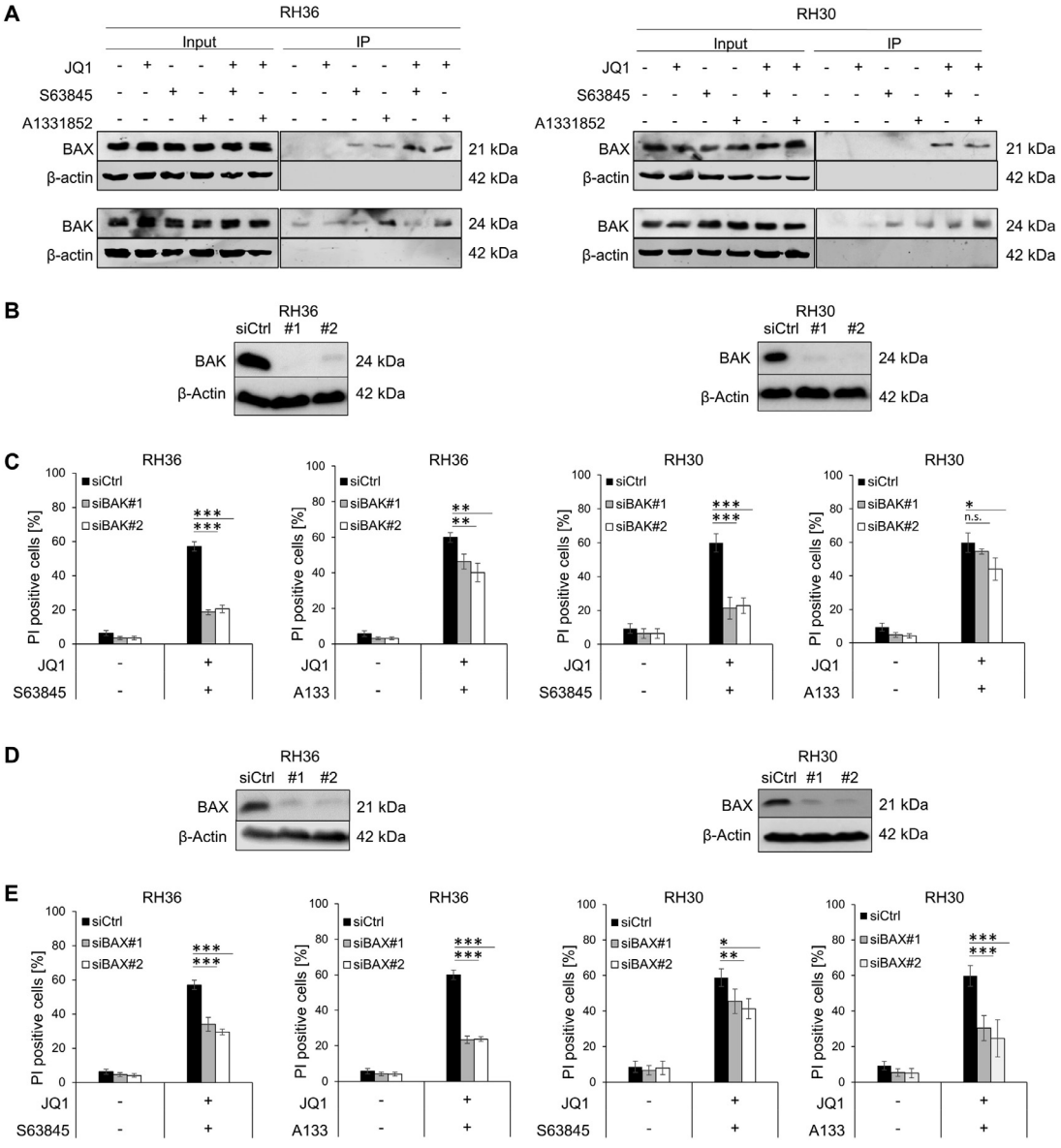

Fig. 4. JQ1/S63845- and JQ1/A-1331852-induced cell death is dependent on BAK and BAX. (A) RH30 and RH36 cells were treated with JQ1 (0.5 μM), A133 (0.25 μM) and/or S63845 (0.25 μM) for 6 h. Activation of BAX and BAK was detected by immunoprecipitation using active conformation specific antibodies for BAK and BAX and protein expression was analyzed by Western blotting. β-Actin served as loading control. Representative blots of two experiments are shown. (B-E) RMS cell lines were transiently transfected with non-silencing siRNA (siCtrl) or with one construct targeting BAK (siBAK-1, siBAK-2) (B, C) and one construct targeting BAX (siBAX-1, siBAX-2) (D, E). Expression levels of BAX and BAK were analyzed by Western blotting, β-Actin served as loading control. Representative blots of at least two independent experiments are shown (B, D). Transiently transfected RMS cell lines were treated with 0.5 μM JQ1 and/or 0.25 μM S63845 (MCL1i) and/or A-1331852 (Bcl-x_Li) for 72 h and apoptosis was determined by analysis of PI/Hoechst staining using the ImageXpress Micro XLS system (C, E). Data represent the mean and SD of three independent experiments, performed in triplicates; $^{*}p<0.05$, $^{**}p<0.01$, $^{***}p<0.001$.

constructs for targeting BIM and NOXA (Figure 6A, 6D). Interestingly, knockdown of BIM significantly rescued RH36 and RH30 cells from JQ1/S63845- and JQ1/A-1331852-mediated apoptosis (Figure 6A, 6B). Genetic silencing of NOXA had no significant effect on JQ1/S63845-mediated apoptosis in RH36 and RH30 cells (Figure 6C, 6D), whereas JQ1/A-1331852-mediated apoptosis was significantly rescued by genetic silencing of NOXA (Figure 6C, 6D). Taken together, BIM is functionally relevant for JQ1/A-1331852- and JQ1/S63845-mediated apoptosis while NOXA is important for JQ1/A-1331852-mediated apoptosis, but not for JQ1/S63845-mediated apoptosis.

To further explore the relevance of the mitochondrial pathway for JQ1/S63845- and JQ1/A-1331852-induced apoptosis, we generated RH36 and RH30 cells stably overexpressing murine BCL-2 protein, known to impair mitochondrial apoptosis (Figure 6E, 6F). Overexpression of murine BCL-2 significantly protected RMS cells against JQ1/S63845- and JQ1/A-1331852-induced apoptosis as observed by PI positive cells, highlighting the relevance of the mitochondrial pathway (Figure 6F). Of note, overexpression of BCL-x_L slightly rescued from JQ1/S63845- and JQ1/A-1331852-induced apoptosis. However, this effect was not significant (Supplementary Figure 4).

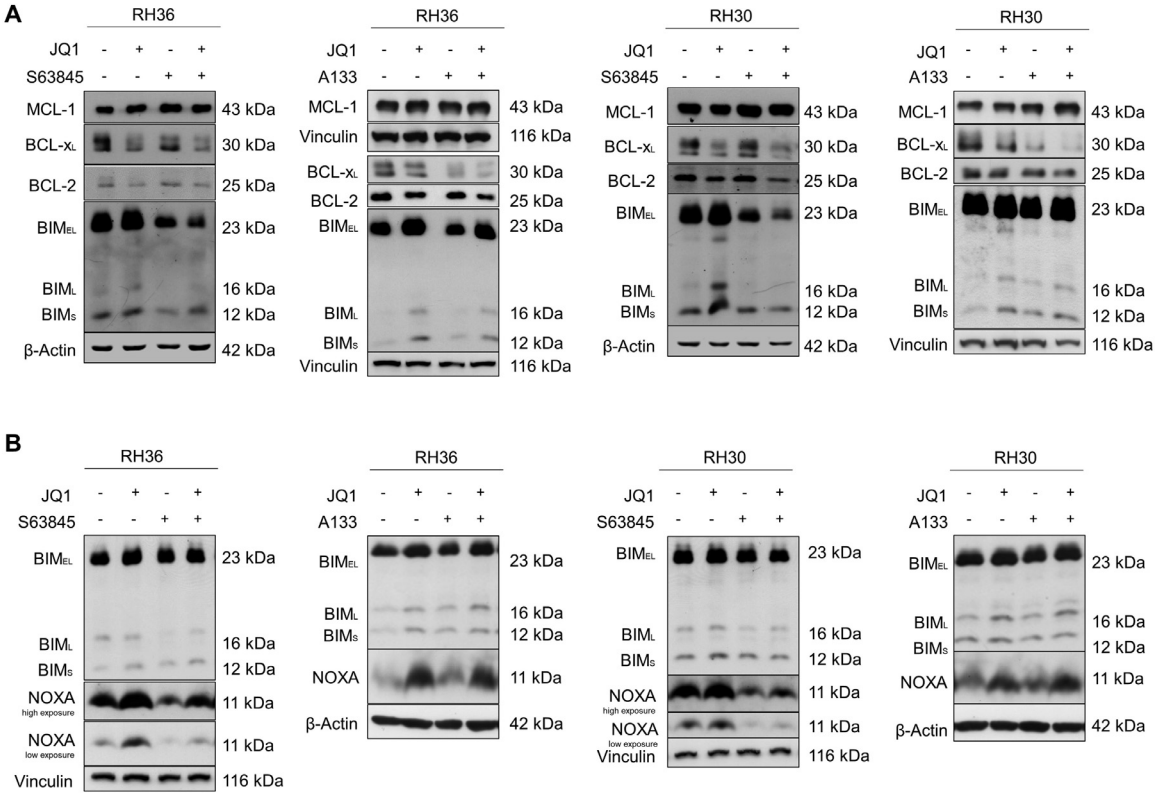

Fig. 5. JQ1/A-1331852 and JQ1/S63845 co-treatment differently regulate BIM and NOXA expression. (A+B) RMS cells were treated with 0.5 μM JQ1 and/or 0.25 μM S63845 (MCL1i) and/or A-1331852 (Bcl-x_Li) for 6 h (A) or 16 h (B) and protein expression was analyzed by Western blotting. GAPDH, Vinculin or *β*-Actin served as loading control. Representative blots of two experiments are shown.

Discussion

In recent years, BH3 mimetics have gained interest as novel cancer therapeutics [15, 25, 26]. BH3 mimetics selectively inhibit BCL-2, BCL-x_L, or MCL-1 (ABT-199, A-1331852, S63845), thereby rebalancing pro- and anti-apoptotic proteins in favor of mitochondrial apoptosis. While BH3 mimetics alone had low efficiency to induce cell death in RMS, several studies have highlighted the potential of BH3 mimetics in combination treatments for treatment of RMS [15, 17].

In this study, we identified a novel synthetic lethal interaction of BH3 mimetics selectively inhibiting the proteins BCL-2, BCL-x_L, or MCL-1 (ABT-199, A-1331852, S63845) and the BET inhibitor JQ1 to induce mitochondrial apoptosis in RMS cells by cooperatively rebalancing of pro- and anti-apoptotic proteins. While former studies were restricted to the investigation of BET inhibition in combination with one BH3 mimetic [27, 28], this is the first study to compare three different BH3 mimetics in combination with JQ1 in RMS cells. The potency of all three combinations was determined by calculation of the Bliss synergy score identifying the combinations of JQ1/S63845 and JQ1/A-1331852 as most synergistic co-treatments. Of note, these combinations exhibited some tumor selectivity, since they have shown negligible effects on non-malignant cells *in vitro*. The potency of JQ1/S63845 and JQ1/A-1331852 co-treatment was further underlined by JQ1/S63845 and JQ1/A-1331852-mediated cooperative inhibition of cell viability, reduction of colony formation and cell death induction in 3D spheroid models.

Next, we identified mitochondrial apoptosis as molecular mechanism of JQ1/S63845 and JQ1/A-1331852-mediated cell death induction as shown by the following experimental results: First, JQ1/S63845 and JQ1/A-1331852 co-treatment rebalanced pro- and anti-apoptotic BCL-2 proteins tightly controlling mitochondrial apoptosis. JQ1 alone upregulated pro-apoptotic BIM and NOXA while downregulating BCL-x_L, thereby rebalancing pro- and anti-apoptotic proteins in favor of apoptosis without inducing cell death in RMS. Additional inhibition of BCL-x_L or MCL-1 enhanced pro-apoptotic rebalancing, resulting in apoptosis. This model is supported by genetic knockdown experiments targeting the pro-apoptotic BIM, significantly rescuing RMS cells from JQ1/S63845- and JQ1/A-1331852-mediated cell death or, vice versa, overexpression of anti-apoptotic BCL-2 significantly rescued RMS cells from JQ1/S63845- and JQ1/A-1331852-mediated cell death. Second, BAK and BAX are crucial for JQ1/S63845- and JQ1/A-1331852-mediated cell death, since genetic silencing of BAK and BAX significantly rescued RMS cells from JQ1/S63845- and JQ1/A-1331852-mediated apoptosis. Third, caspase activation is necessary for JQ1/S63845 and JQ1/A-1331852-mediated apoptosis, since inhibition of caspases by the broad range caspase inhibitor zVAD.fmk significantly reduced JQ1/S63845- and JQ1/A-1331852-mediated DNA fragmentation. Taken together, these results indicate a crucial role of the mitochondrial pathway for JQ1/S63845- and JQ1/A-1331852-mediated apoptosis in RMS cells. These results go in line with previous studies characterizing the mitochondrial pathway as mechanism for cell death execution upon the combination of JQ1 with BH3 mimetics [27, 28].

Moreover, we identify JQ1/S63845 and JQ1/A-1331852 co-treatment as the most potent combinations and highlighted different contributions of NOXA, BAK and BAX for JQ1/S63845- and JQ1/A-1331852-mediated apoptosis for the first time. S63845 or JQ1/S63845 co-treatment increased MCL-1 and decreased BIM and NOXA protein levels. Increased MCL-1 levels upon S63845 treatment can be explained by binding of S63845 to MCL-1 stabilizing MCL-1 [18]. Binding of BIM to BCL-2, BCL-x_L and

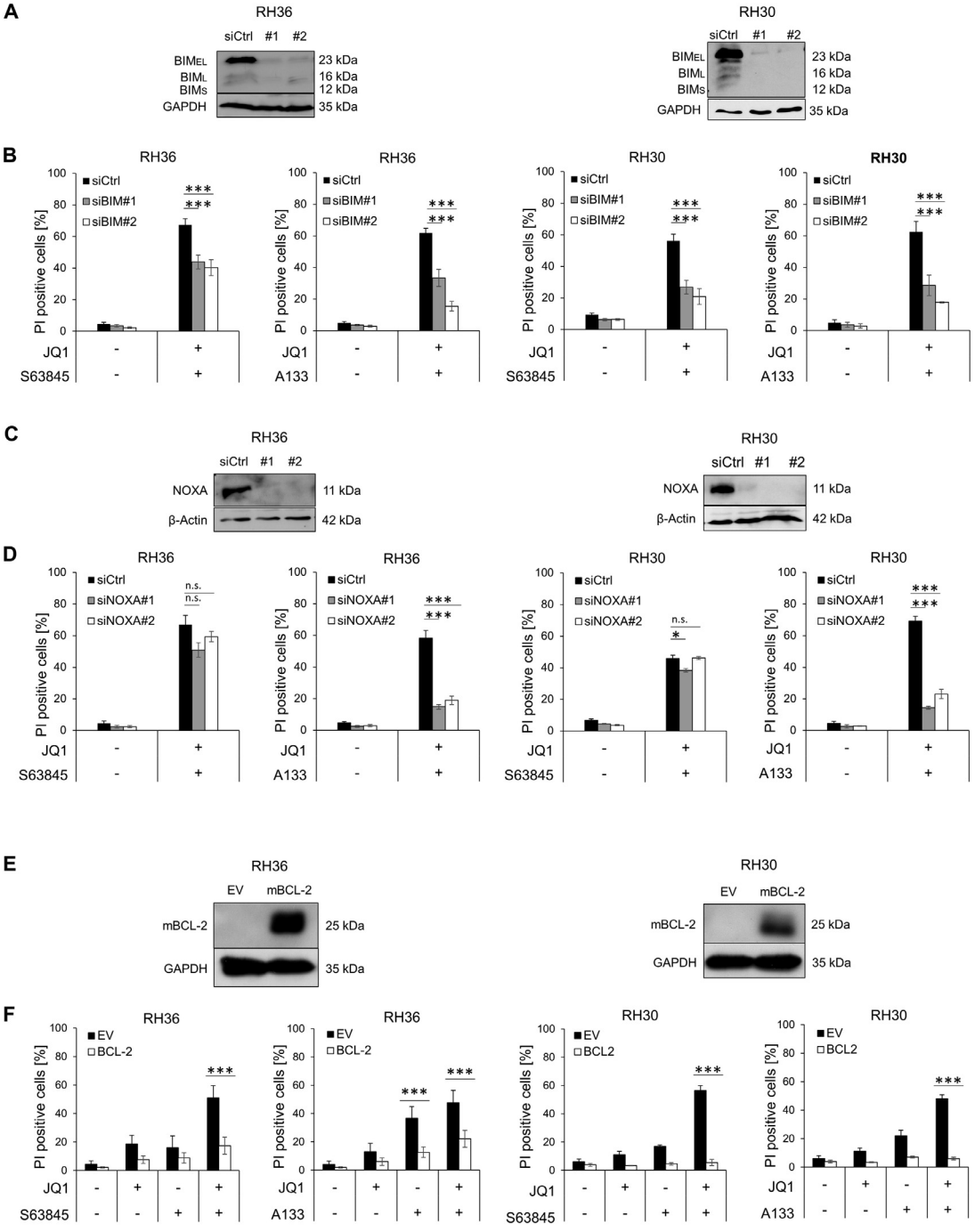

Fig. 6. JQ1/A-1331852- and JQ1/S63845-mediated apoptosis is dependent on proapoptotic rebalancing of BCL-2 proteins. (A-D) RMS cell lines were transiently transfected with non-silencing siRNA (siCtrl) or with two constructs targeting BIM (siBIM-1, siBIM-2) and two constructs targeting NOXA (siNOXA-1, siNOXA-2). (A, C) Expression levels of BIM and NOXA were analyzed by Western blotting, GAPDH or β-Actin served as loading controls. Representative blots of at least two independent experiments are shown. (B, D) Transiently transfected RMS cell lines were treated with 0.5 µM JQ1 and/or 0.25 µM S63845 (MCL1i) and/or A-1331852 (Bcl-x_Li) for 72 h and apoptosis was determined by analysis of PI/Hoechst staining and ImageXpress Micro XLS system. (E, F) RMS cells were transfected with murine BCL-2 or EV and expression of BCL-2 was assessed by Western blotting, GAPDH served as loading controls. (E) RMS cells were treated with 0.5 µM JQ1 and/or 0.25 µM S63845 (MCL1i) and/or A-1331852 (Bcl-x_Li) for 72 h and apoptosis was determined by analysis of PI/Hoechst staining using the ImageXpress Micro XLS system. Data represent the mean ± SD of three independent experiments, performed in triplicates; $^{*}p<0.05$, $^{**}p<0.01$, $^{***}p<0.001$.

MCL-1 as well as binding of NOXA to MCL-1 results in stabilization of BIM and NOXA [12, 15, 29]. Upon S63845 or JQ1/S63845 treatment, BIM and NOXA are displaced from MCL-1 and degraded, explaining the decreased BIM levels after 16 hours and decreased NOXA protein levels after 6 hours upon S63845 and JQ1/S63845 treatment. The effect of MCL-1 inhibition on protein degradation of NOXA appears earlier compared to BIM, since NOXA is exclusively bound to MCL-1 and a short-life protein being rapidly degraded [29]. Since NOXA is already degraded upon JQ1/S63845 co-treatment, siRNA-mediated knockdown of NOXA was not able to rescue from JQ1/S63845-mediated apoptosis. By comparison, A-1331852 and JQ1/A-1331852 co-treatment reduced BCL-x_L protein levels after 16 hours, but did not affect JQ1-mediated NOXA induction since NOXA is still bound to MCL-1. In consequence, NOXA contributed to JQ1/A-1331852-mediated apoptosis as indicated by siRNA knockdown of NOXA, significantly rescuing RMS cells from JQ1/A-1331852-mediated apoptosis. The cooperative effect of JQ1/A-1331852 and JQ1/S63845 co-treatment on increasing protein levels of activated BAX as well as the significant effect of BAX knockdown rescuing JQ1/A-1331852 and JQ1/S63845-induced apoptosis underline the relevance of BAX for apoptosis induction upon both co-treatments. By comparison, BAK knockdown was more effective rescuing JQ1/S63845 compared to JQ1/A-1331852-induced apoptosis. Differences among the binding interactions of BAK and BAX to BCL-x_L and MCL-1 may also explain why genetic silencing of BAK was more efficient rescuing JQ1/S63845-mediated apoptosis compared to BAX. Since MCL-1 preferably binds BAK, which is no longer neutralized by MCL-1 upon S63845 treatment, JQ1/S63845-mediated apoptosis is more dependent on BAK compared to BAX [30–32]. The minor effects of BCL-x_L overexpression on rescuing JQ1/A-1331852 and JQ1/S63845-mediated apoptosis could be caused by limited overexpression efficiency and relatively high intrinsic BCL-x_L levels resulting in minor effects of additionally expressed BCL-x_L or by a cell line dependent difference in the effectiveness of BCL-2 and BCL-x_L rescuing apoptosis as previously described for other tumor entities [33]. Previous studies have elucidated BH3 mimetics as efficient drugs in combination therapies in RMS [15, 17]. However, platelet toxicity limited the use of BCL-x_L inhibitors [34]. MCL-1 inhibitors appeared in first instance to be better tolerated [12], however, the efficiency of all BH3 mimetics is limited by resistance mechanisms such as compensatory upregulation of other anti-apoptotic BCL-2 proteins [35]. This aquired chemoresistance is frequently mediated by transcriptional plasticity and generation of *de novo* super enhancers, which are highly dependent on BRD4 [36, 37]. By inhibiting BRD4, BET inhibitors disrupt transcriptional adaptive responses and overcome chemoresistance [38]. Besides, BET inhibition rebalances BCL-2 proteins in favor of apoptosis thereby sensitizing cells towards apoptosis [6, 28]. Here, we show that JQ1 and BH3 mimetics potently synergize to induce mitochondrial apoptosis in RMS cells.

BET inhibitors (NCT03936465) as well as the MCL-1 and BCL-x_L inhibitors have entered clinical trials (NCT02979366, NCT02992483, NCT01633541), highlighting their potential for clinical usage. With regard to the limited therapeutic window of BH3 mimetics and the risk of fast adaptive responses, combination of BH3 mimetics and BET inhibitors occurs as a compelling new strategy for the treatment of RMS patients. Taken together, this study highlights the potential of BH3 mimetics in combination with the BET inhibitor JQ1 inducing mitochondrial apoptosis in RMS cells providing an important rationale to transfer combinations of BH3 mimetics and BET inhibitors into clinical application for the treatment of RMS.

Declaration of Competing Interest

None to declare.

Acknowledgments

This work was supported by grants from the Mildred-Scheel-Nachwuchszentrum Frankfurt (70113301) funded by the Deutsche Krebshilfe e.V. (to UE). Further, this work was supported by the SGC (to S.K., M.W.), a registered charity (no: 1097737) that receives funds from AbbVie, Bayer AG, Boehringer Ingelheim, Canada Foundation for Innovation, Eshelman Institute for Innovation, Genentech, Genome Canada through Ontario Genomics Institute [OGI-196], EU/EFPIA/OICR/McGill/KTH/Diamond, Innovative Medicines Initiative 2 Joint Undertaking [EUbOPEN grant 875510], Janssen, Merck KGaA (aka EMD in Canada and US), Merck & Co (aka MSD outside Canada and US), Pfizer, São Paulo Research Foundation-FAPESP, Takeda and Wellcome [106169/ZZ14/Z].

Author contributions

UE, SL and CB performed experiments and analyzed data. ND and CB discussed data and manuscript. ND and VS performed the experiments for the revision. CB and ND designed the project. CB wrote the manuscript with support of all other co-authors. SK and MW synthesized the JQ1 inhibitor. ND, SK, MW, SL, MTM contributed to revising the manuscript. All the authors agreed to be accountable for the content of the work.

References

[1] De Giovanni C, Landuzzi L, Nicoletti G, Lollini PL, Nanni P. Molecular and cellular biology of rhabdomyosarcoma. *Future Oncol* 2009;**5**:1449–75.

[2] Breneman JC, Lyden E, Pappo AS, Link MP, Anderson JR, Parham DM, Qualman SJ, Wharam MD, Donaldson SS, Maurer HM, Meyer WH, Baker KS, Paidas CN, Crist WM. Prognostic factors and clinical outcomes in children and adolescents with metastatic rhabdomyosarcoma–a report from the Intergroup Rhabdomyosarcoma Study IV. *J Clin Oncol* 2003;**21**:78–84.

[3] Filippakopoulos P, Qi J, Picaud S, Shen Y, Smith WB, Fedorov O, Morse EM, Keates T, Hickman TT, Felletar I, Philpott M, Munro S, McKeown MR, Wang Y, Christie AL, West N, Cameron MJ, Schwartz B, Heightman TD, Thangue NLa, French CA, Wiest O, Kung AL, Knapp S, Bradner JE. Selective inhibition of BET bromodomains. *Nature* 2010;**468**:1067–73.

[4] Delmore JE, Issa GC, Lemieux ME, Rahl PB, Shi J, Jacobs HM, Kastritis E, Gilpatrick T, Paranal RM, Qi J, Chesi M, Schinzel AC, McKeown MR, Heffernan TP, Vakoc CR, Bergsagel PL, Ghobrial IM, Richardson PG, Young RA, Hahn WC, Anderson KC, Kung AL, Bradner JE, Mitsiades CS. BET bromodomain inhibition as a therapeutic strategy to target c-Myc. *Cell* 2011;**146**:904–17.

[5] Gerlach D, Tontsch-Grunt U, Baum A, Popow J, Scharn D, Hofmann MH, Engelhardt H, Kaya O, Beck J, Schweifer N, Gerstberger T, Zuber J, Savarese F, Kraut N. The novel BET bromodomain inhibitor BI 894999 represses super-enhancer-associated transcription and synergizes with CDK9 inhibition in AML. *Oncogene* 2018;**37**:2687–701.

[6] Boedicker C, Hussong M, Grimm C, Dolgikh N, Meister MT, Enssle JC, Wanior M, Knapp S, Schweiger MR, Fulda S. Co-inhibition of BET proteins and PI3Kalpha triggers mitochondrial apoptosis in rhabdomyosarcoma cells. *Oncogene* 2020;**39**:3837–52.

[7] Tan Z, Zhang X, Kang T, Zhang L, Chen S. Arsenic sulfide amplifies JQ1 toxicity via mitochondrial pathway in gastric and colon cancer cells. *Drug Des Devel Ther* 2018;**12**:3913–27.

[8] Fiskus W, Cai T, DiNardo CD, Kornblau SM, Borthakur G, Kadia TM, Pemmaraju N, Bose P, Masarova L, Rajapakshe K, Perera D, Coarfa C, Mill CP, Saenz DT, Saenz DN, Sun B, Khoury JD, Shen Y, Konopleva M, Bhalla KN. Superior efficacy of cotreatment with BET protein inhibitor and BCL2 or MCL1 inhibitor against AML blast progenitor cells. *Blood Cancer J* 2019;**9**:4.

[9] Fulda S, Debatin KM. Targeting apoptosis pathways in cancer therapy. *Curr Cancer Drug Targets* 2004;**4**:569–76.

[10] Gross A, McDonnell JM, Korsmeyer SJ. BCL-2 family members and the mitochondria in apoptosis. *Genes Dev* 1999;**13**:1899–911.

[11] Chen L, Willis SN, Wei A, Smith BJ, Fletcher JI, Hinds MG, Colman PM, Day CL, Adams JM, Huang DC. Differential targeting of prosurvival Bcl-2 proteins by their BH3-only ligands allows complementary apoptotic function. *Mol Cell* 2005;**17**:393–403.

[12] Kotschy A, Szlavik Z, Murray J, Davidson J, Maragno AL, Le Toumelin-Braizat G, Chanrion M, Kelly GL, Gong JN, Moujalled DM, Bruno A, Csekei M, Paczal A, Szabo ZB, Sipos S, Radics G, Proszenyak A, Balint B, Ondi L, Blasko G, Robertson A, Surgenor A, Dokurno P, Chen I, Matassova N, Smith J, Pedder C, Graham C, Studeny A, Lysiak-Auvity G, Girard AM, Grave F, Segal D, Riffkin CD, Pomilio G, Galbraith LC, Aubrey BJ, Brennan MS, Herold MJ, Chang C, Guasconi G, Cauquil N, Melchiore F, Guigal-Stephan N, Lockhart B, Colland F, Hickman JA, Roberts AW, Huang DC, Wei AH, Strasser A, Lessene G, Geneste O. The MCL1 inhibitor S63845 is tolerable and effective in diverse cancer models. *Nature* 2016;**538**:477–82.

[13] Oltersdorf T, Elmore SW, Shoemaker AR, Armstrong RC, Augeri DJ, Belli BA, Bruncko M, Deckwerth TL, Dinges J, Hajduk PJ, Joseph MK, Kitada S, Korsmeyer SJ, Kunzer AR, Letai A, Li C, Mitten MJ, Nettesheim DG, Ng S, Nimmer PM, O'Connor JM, Oleksijew A, Petros AM, Reed JC, Shen W, Tahir SK, Thompson CB, Tomaselli KJ, Wang B, Wendt MD, Zhang H, Fesik SW, Rosenberg SH. An inhibitor of Bcl-2 family proteins induces regression of solid tumours. *Nature* 2005;**435**:677–81.

[14] Souers AJ, Leverson JD, Boghaert ER, Ackler SL, Catron ND, Chen J, Dayton BD, Ding H, Enschede SH, Fairbrother WJ, Huang DC, Hymowitz SG, Jin S, Khaw SL, Kovar PJ, Lam LT, Lee J, Maecker HL, Marsh KC, Mason KD, Mitten MJ, Nimmer PM, Oleksijew A, Park CH, Park CM, Phillips DC, Roberts AW, Sampath D, Seymour JF, Smith ML, Sullivan GM, Tahir SK, Tse C, Wendt MD, Xiao Y, Xue JC, Zhang H, Humerickhouse RA, Rosenberg SH, Elmore SW. ABT-199, a potent and selective BCL-2 inhibitor, achieves antitumor activity while sparing platelets. *Nat Med* 2013;**19**:202–8.

[15] Kehr S, Haydn T, Bierbrauer A, Irmer B, Vogler M, Fulda S. Targeting BCL-2 proteins in pediatric cancer: dual inhibition of BCL-XL and MCL-1 leads to rapid induction of intrinsic apoptosis. *Cancer Lett* 2020;**482**:19–32.

[16] Yecies D, Carlson NE, Deng J, Letai A. Acquired resistance to ABT-737 in lymphoma cells that up-regulate MCL-1 and BFL-1. *Blood* 2010;**115**:3304–13.

[17] Heinicke U, Haydn T, Kehr S, Vogler M, Fulda S. BCL-2 selective inhibitor ABT-199 primes rhabdomyosarcoma cells to histone deacetylase inhibitor-induced apoptosis. *Oncogene* 2018;**37**:5325–39.

[18] Li Z, He S, Look AT. The MCL1-specific inhibitor S63845 acts synergistically with venetoclax/ABT-199 to induce apoptosis in T-cell acute lymphoblastic leukemia cells. *Leukemia* 2019;**33**:262–6.

[19] Enssle JC, Boedicker C, Wanior M, Vogler M, Knapp S, Fulda S. Co-targeting of BET proteins and HDACs as a novel approach to trigger apoptosis in rhabdomyosarcoma cells. *Cancer Lett* 2018;**428**:160–72.

[20] Heinicke U, Fulda S. Chemosensitization of rhabdomyosarcoma cells by the histone deacetylase inhibitor SAHA. *Cancer Lett* 2014;**351**:50–8.

[21] Fulda S, Sieverts H, Friesen C, Herr I, Debatin KM. The CD95 (APO-1/Fas) system mediates drug-induced apoptosis in neuroblastoma cells. *Cancer Res* 1997;**57**:3823–9.

[22] Merker M, Pfirrmann V, Oelsner S, Fulda S, Klingebiel T, Wels WS, Bader P, Rettinger E. Generation and characterization of ErbB2-CAR-engineered cytokine-induced killer cells for the treatment of high-risk soft tissue sarcoma in children. *Oncotarget* 2017;**8**:66137–53.

[23] Schindelin J, Arganda-Carreras I, Frise E, Kaynig V, Longair M, Pietzsch T, Preibisch S, Rueden C, Saalfeld S, Schmid B, Tinevez JY, White DJ, Hartenstein V, Eliceiri K, Tomancak P, Cardona A. Fiji: an open-source platform for biological-image analysis. *Nat Methods* 2012;**9**:676–82.

[24] Ianevski A, He L, Aittokallio T, Tang J. SynergyFinder: a web application for analyzing drug combination dose-response matrix data. *Bioinformatics* 2017;**33**:2413–15.

[25] Anderson MA, Deng J, Seymour JF, Tam C, Kim SY, Fein J, Yu L, Brown JR, Westerman D, Si EG, Majewski IJ, Segal D, Heitner Enschede SL, Huang DC, Davids MS, Letai A, Roberts AW. The BCL2 selective inhibitor venetoclax induces rapid onset apoptosis of CLL cells in patients via a TP53-independent mechanism. *Blood* 2016;**127**:3215–24.

[26] Del Gaizo Moore V, Brown JR, Certo M, Love TM, Novina CD, Letai A. Chronic lymphocytic leukemia requires BCL2 to sequester prodeath BIM, explaining sensitivity to BCL2 antagonist ABT-737. *J Clin Invest* 2007;**117**:112–21.

[27] Peirs S, Frismantas V, Matthijssens F, Van Loocke W, Pieters T, Vandamme N, Lintermans B, Dobay MP, Berx G, Poppe B, Goossens S, Bornhauser BC, Bourquin JP, Van Vlierberghe P. Targeting BET proteins improves the therapeutic efficacy of BCL-2 inhibition in T-cell acute lymphoblastic leukemia. *Leukemia* 2017;**31**:2037–47.

[28] Ishida CT, Bianchetti E, Shu C, Halatsch ME, Westhoff MA, Karpel-Massler G, Siegelin MD. BH3-mimetics and BET-inhibitors elicit enhanced lethality in malignant glioma. *Oncotarget* 2017;**8**:29558–73.

[29] Pang X, Zhang J, Lopez H, Wang Y, Li W, O'Neill KL, Evans JJ, George NM, Long J, Chen Y, Luo X. The carboxyl-terminal tail of Noxa protein regulates the stability of Noxa and Mcl-1. *J. Biol. Chem.* 2014;**289**:17802–11.

[30] Zhai D, Jin C, Huang Z, Satterthwait AC, Reed JC. Differential regulation of Bax and Bak by anti-apoptotic Bcl-2 family proteins Bcl-B and Mcl-1. *J Biol Chem* 2008;**283**:9580–6.

[31] Billen LP, Kokoski CL, Lovell JF, Leber B, Andrews DW. Bcl-XL inhibits membrane permeabilization by competing with Bax. *PLoS Biol* 2008;**6**:e147.

[32] Lee EF, Grabow S, Chappaz S, Dewson G, Hockings C, Kluck RM, Debrincat MA, Gray DH, Witkowski MT, Evangelista M, Pettikiriarachchi A, Bouillet P, Lane RM, Czabotar PE, Colman PM, Smith BJ, Kile BT, Fairlie WD. Physiological restraint of Bak by Bcl-xL is essential for cell survival. *Genes Dev* 2016;**30**:1240–50.

[33] Fiebig AA, Zhu W, Hollerbach C, Leber B, Andrews DW. Bcl-XL is qualitatively different from and ten times more effective than Bcl-2 when expressed in a breast cancer cell line. *BMC Cancer* 2006;**6**:213.

[34] Schoenwaelder SM, Jarman KE, Gardiner EE, Hua M, Qiao J, White MJ, Josefsson EC, Alwis I, Ono A, Willcox A, Andrews RK, Mason KD, Salem HH, Huang DC, Kile BT, Roberts AW, Jackson SP. Bcl-xL-inhibitory BH3 mimetics can induce a transient thrombocytopathy that undermines the hemostatic function of platelets. *Blood* 2011;**118**:1663–74.

[35] Davids MS, Deng J, Wiestner A, Lannutti BJ, Wang L, Wu CJ, Wilson WH, Brown JR, Letai A. Decreased mitochondrial apoptotic priming underlies stroma-mediated treatment resistance in chronic lymphocytic leukemia. *Blood* 2012;**120**:3501–9.

[36] Beroukhim R, Mermel CH, Porter D, Wei G, Raychaudhuri S, Donovan J, Barretina J. The landscape of somatic copy-number alteration across human cancers. *Nature* 2010;**463**:899–905.

[37] Ma Q, Yang F, Mackintosh C, Jayani RS, Oh S, Jin C, Nair SJ, Merkurjev D, Ma W, Allen S, Wang D, Almenar-Queralt A, Garcia-Bassets I. Super-enhancer redistribution as a mechanism of broad gene dysregulation in repeatedly drug-treated cancer cells. *Cell Rep* 2020;**31**:107532.

[38] Stratikopoulos EE, Dendy M, Szabolcs M, Khaykin AJ, Lefebvre C, Zhou MM, Parsons R. Kinase and BET inhibitors together clamp inhibition of PI3K signaling and overcome resistance to therapy. *Cancer Cell* 2015;**27**:837–51.